Stochastic Forcing of Potential Vorticity: Observations

JOSEPH EGGER

Meteorologisches Institut, Universität München, Munich, Germany

KLAUS-PETER HOINKA

Institut für Physik der Atmosphäre, DLR, Oberpfaffenhofen, Germany

(Manuscript received 26 August 2010, in final form 17 January 2011)

ABSTRACT

The linear theory of point correlation maps for synoptic systems relies so far mainly on specifications of stochastic forcing due to nonlinear processes that are not based on observations. Forty-year ECMWF Re-Analysis (ERA-40) data are used to derive time series of the forcing terms in a potential vorticity equation for a correlation point in the North Atlantic storm-track region. It is found that the forcing correlations are restricted to distances less than 1500 km to the correlation point in zonal direction and just a few hundred kilometers in meridional direction. The forcing is not even approximately white in time. Covariances of forcing and potential vorticity are presented as well. An advection equation with simple damping and realistic stochastic forcing is solved to approximate the observed covariances of forcing and potential vorticity.

1. Introduction

By now, the statistical features of extratropical weather systems have been explored in some detail (e.g., Hoskins and Hodges 2002, and references therein). We are informed about the location of the storm tracks, the related transports of momentum and heat, and the changes of eddy statistics with lag. As demonstrated by Blackmon et al. (1984) and many others, the correlations of heights at a reference point and all other points form a wave pattern at lag $\tau = 0$ with decay of the wave amplitudes upstream and downstream. This pattern is normally moving eastward, intensifies with increasing negative lag, and becomes weaker for positive increasing lag. An example is presented in Fig. 1 where potential vorticity (PV)

$$q = \rho^{-1}(\zeta + f)\frac{\partial \theta}{\partial z} \tag{1.1}$$

is selected as a variable with density ρ, vorticity ζ, potential temperature θ, and Coriolis parameter f. The data evaluation is based on the 40-yr European Centre for Medium-Range Weather Forecasts (ECMWF) Re-Analysis (ERA-40) data (see section 2). Although q is not strictly conserved in adiabatic and frictionless flow, the deviations of q from the correct formulation in isentropic coordinates are too small to be of interest here. Let us denote by $C(b, c|\tau)$ the covariance of variable b and variable c where b leads with lag τ. Figure 1 shows the regression $C(\hat{q}, q|0)\sigma_{\hat{q}}^{-1}$ of $q = \hat{q}$ at the correlation point (dot in Fig. 1) and PV at all other points at the constant height surface $z = 8$ km where $\sigma_{\hat{q}}$ is the standard deviation of $\hat{q}$. There is an elliptic domain of positive covariances with "radius" ~1000 km centered at the correlation point. Domains with negative correlations are found in the east and west. There are also high covariance values at levels above the correlation point while the amplitude decreases downward (not shown).

A theoretical investigation of Fig. 1 has to start from the PV equation

$$\frac{\partial}{\partial t}q' + \nabla \cdot (\overline{\mathbf{v}}q' + \mathbf{v}'\overline{q} + \mathbf{v}'q') = -dq' \tag{1.2}$$

with three-dimensional velocity $\mathbf{v} = (u, v, w)$, where the overbar denotes the time mean state and the prime deviations from the mean. It is assumed in (1.2) that the flow is incompressible and that dissipative effects can be represented by a simple damping term. Forcing by

Corresponding author address: Joseph Egger, Meteorological Institute, University of Munich, Theresienstr. 37, 80333 Munich, Germany.
E-mail: j.egger@lrz.uni-muenchen.de

DOI: 10.1175/2011JAS3654.1

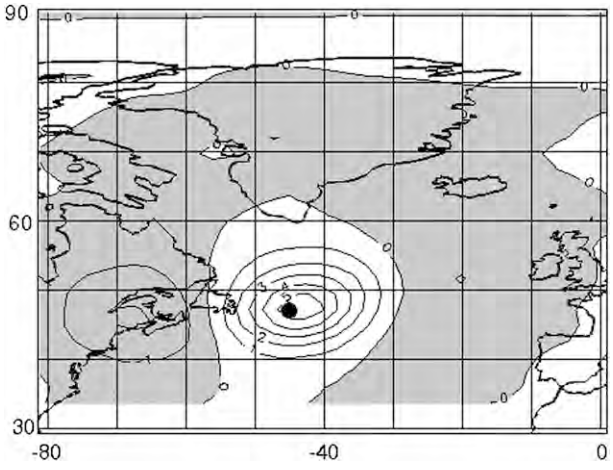

FIG. 1. Normalized covariance $C(\hat{q}, q|\tau)$ in 0.2 PVU of the potential vorticity $\hat{q}$ at the correlation point (dot) with q at the level $z = 8$ km and for lag $\tau = 0$. Negative values are shaded.

heating is excluded. The deviations contain all available time scales.

Multiplication of (1.2) by $\hat{q}$ yields, after simple manipulations and after taking expectations, the following:

$$\frac{\partial}{\partial\tau}C(\hat{q}, q|\tau) + \nabla\cdot[\overline{\mathbf{v}}C(\hat{q}, q|\tau) + \overline{q}C(\hat{q}, \mathbf{v}|\tau)] + C[\hat{q}, \nabla\cdot(\mathbf{v}'q')|\tau] = -dC(\hat{q}, q|\tau). \quad (1.3)$$

To solve (1.3) one has to "invert" $C(\hat{q}, q|\tau)$, that is, to derive $C(\hat{q}, \mathbf{v}|\tau)$ invoking boundary conditions and a balance constraint. The main problem, of course, is posed by the last term on the left-hand side, namely the covariance of $\hat{q}$ and the eddy flux of PV. Various efforts to tackle this problem have been made for some time. Egger and Schilling (1984) dealt with the barotropic normal mode version of (1.3) and used data to determine the forcing based on a scale separation (see also Metz 1986). They found that the nonlinear term has a fairly complicated statistical structure that varies from mode to mode. These results cannot readily be extended to the baroclinic flows in physical space addressed by (1.3). We are, however, not aware of further attempts to derive the statistical characteristics of the nonlinear eddy terms in (1.3) from data. Instead, assumptions are made. For example, Farrell and Ioannou (2009) represent this term as noise that is white in space and time but adjust also the damping in a two-layer model (see also DelSole and Farrell 1995). Whitaker and Sardeshmukh (1998) implemented a white noise forcing in a hemispheric two-level model and found that the observed point-correlation maps can be reproduced quite well [see also Newman et al. (1997) for the corresponding barotropic problem]. Farrell and Ioannou (2009) force locally while Whitaker and Sardesmukh (1998) drive streamfunction modes. These results suggest that the structure of the observed streamfunction correlation maps is mainly determined by the interactions of the perturbations with the mean flow while the specification of the forcing may be of secondary importance.

On the other hand, Frederiksen and Kepert (2006) and Zidikheri and Frederiksen (2010a,b) used data from numerical simulations to represent the contributions from subgrid motions to the nonlinear eddy terms in a quasigeostrophic model. A specific linear model that includes white noise forcing is used for these contributions. Thus, a fairly detailed treatment of the forcing was found to be necessary for successful simulations. Jin et al. (2006a,b) demonstrated that the vorticity transports by synoptic eddies can be modeled on the basis of the so-called synoptic eddy and low-frequency flow (SELF) closure.

Further progress in the field may profit from information based on data. It is the purpose of this paper to explore the statistical characteristics of the nonlinear term in (1.3) by considering the situation for the correlation point in Fig. 1.

2. Observed forcing characteristics

Time series of the spherical forcing

$$F = -\left[\frac{1}{a\cos\varphi}\frac{\partial}{\partial\lambda}(u'q') + \frac{1}{a\cos\varphi}\frac{\partial}{\partial\varphi}(\cos\varphi v'q') + \frac{1}{\overline{\rho}}\frac{\partial}{\partial z}(\overline{\rho}w'q')\right] \quad (2.1)$$

are calculated on the basis of the ERA-40 analyses for the years 1958–2001 where λ is longitude, φ is latitude, a is the earth's radius, and the mean density is $\overline{\rho}$. The negative sign in (2.1) implies that the forcing is written on the right-hand side of (1.2). The forcing is evaluated from a grid point representation of the ERA-40 data in height coordinates with a vertical distance $Dz = 1000$ m and for a horizontal mesh of 2.5° × 2.5°. The values of F are calculated at all grid points as daily means. The correlation point P is located in the North Atlantic storm-track region (47.5°N, 45.0°W) at a height $z = 8$ km. Note that the forcing contains all time scales. It is left for further work to introduce various filters. On the other hand, (1.2) does not contain any preference for a time scale. Of course, the forcing has to be adapted to the model where it is incorporated. A model for slow dynamics needs forcing by fast motions only.

Figure 2 shows the normalized covariance $C(\hat{F}, F|\tau)$ at the height of the correlation point (dot in Fig. 2a) for (a) $\tau = -1$, (b) $\tau = 0$, and (c) $\tau = 1$ day. The basic pattern at

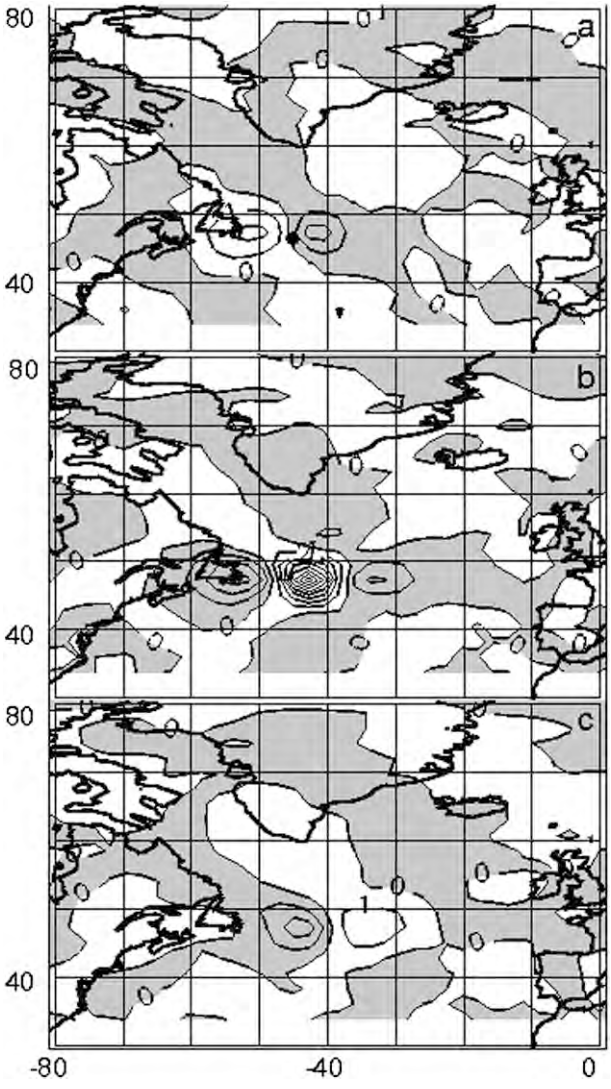

FIG. 2. Normalized covariance $C(\hat{F}, F|\tau)$ of the forcing $\hat{F}$ [see (2.1)] at the correlation point [dot in (a)] with the forcing F at the level $z = 8$ km in 0.5 PVU day^{-1} for (a) $\tau = -1$, (b) $\tau = 0$, and (c) $\tau = 1$ day. Negative values are shaded.

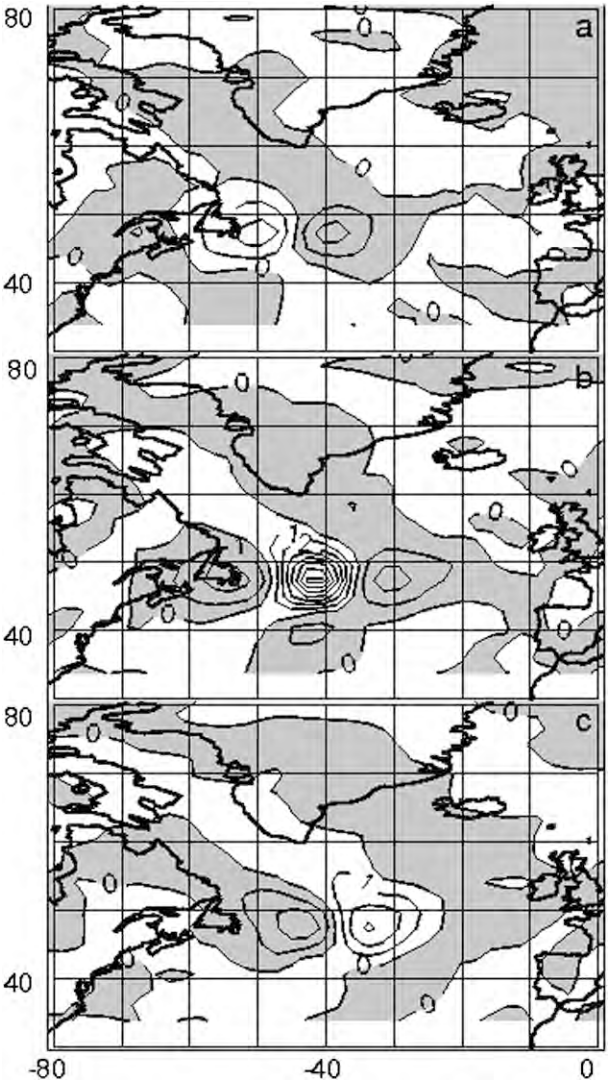

FIG. 3. As in Fig. 2, but at $z = 10$ km. Normalized covariances are in 0.5 PVU day^{-1}.

$\tau = 0$ consists of a domain of positive values centered at P with negative areas in the east and west. This forcing is quite strong with a maximum of ~4 PVU day^{-1} (1 PVU = 10^{-6} m^2 K s^{-1} kg^{-1}). The zonal extent of this positive domain is ~500 km; the meridional one is somewhat less. There are weak indications of a wave pattern in meridional direction. A simple dynamical explanation of this structure is not available. For example, unstable Eady waves are generally accepted as simple models of active baroclinic systems but $F = 0$ for these modes because their perturbation PV vanishes. The pattern moves eastward with a speed of ~5 m s^{-1}. There is rapid increase from $\tau = -1$ to $\tau = 0$ days and equally rapid decay for positive lag. These rapid changes, however, do not continue with increasing $|\tau|$. Appreciable covariances are found for lags of a few days. For example, $C(\hat{F}, \hat{F}, \tau)/\sigma_{\hat{F}} = 4.2$ PVU day^{-1} at $\tau = 0$, but the value of -0.86 (-0.9) for $\tau = -2$ (2) days is almost as large as for $\tau = -1$ (1) day. It is likely that this tail of the decay is due to the interaction between synoptic eddy and low-frequency variability (e.g., Jin et al. 2006a,b).

The covariance $C(\hat{F}, F|\tau)$ at $z = 10$ km (Fig. 3) is quite similar to that at $z = 8$ km in Fig. 2. The same is true at $z = 6$ km except that the amplitudes are less than one-tenth of those in Fig. 2 (not shown). There is a clear signal even at $z = 4$ km (Fig. 4) although the amplitudes are quite small. No appreciable covariances are found at

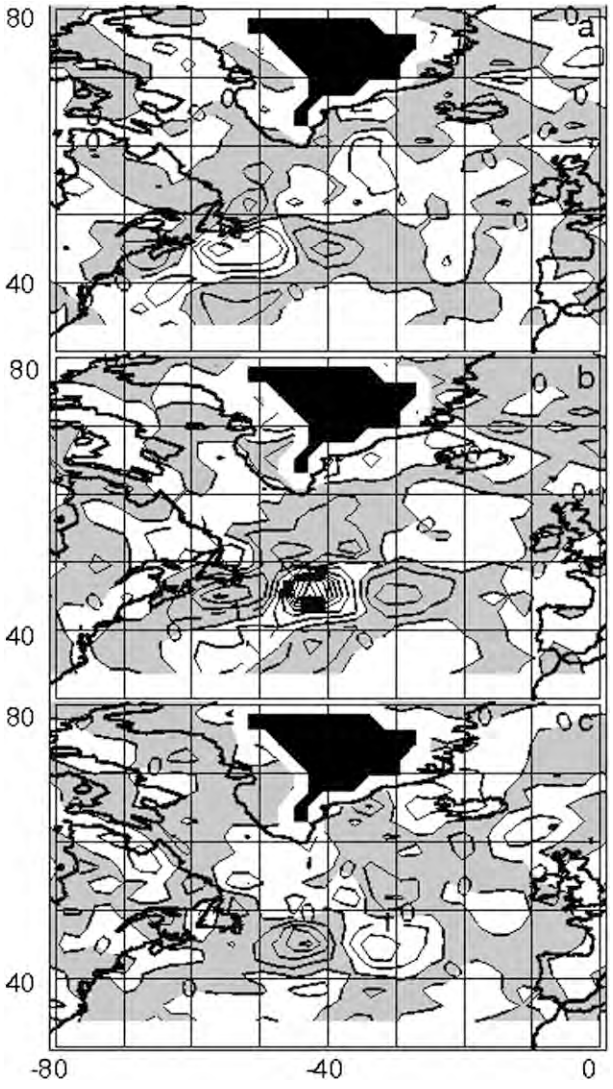

FIG. 4. As in Fig. 2, but at $z = 4$ km. Normalized covariances are in 0.02 PVU day^{-1}. Black areas indicate no data.

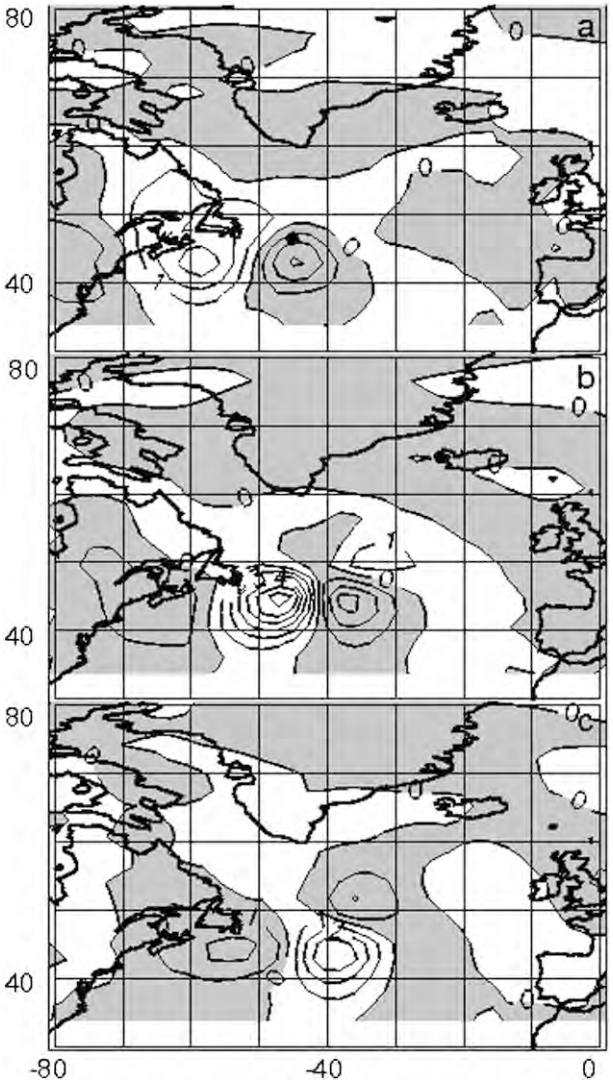

FIG. 5. Normalized covariance $C(\hat{F}, q|\tau)$ of the forcing $\hat{F}$ at the correlation point [dot in (a)] with PV at $z = 8$ km in 0.05 PVU for (a) $\tau = -1$, (b) $\tau = 0$, and (c) $\tau = 1$ day. Negative values shaded.

$z = 2$ km (not shown). Altogether it is seen that the covariance $C(\hat{F}, F|\tau)$ extends through most of the troposphere with little change of the pattern in the vertical. The forcing is not even approximately white in time and has a wavy pattern in zonal direction. It has a coherent time–space propagation, partly in support of the modeling assumptions in Jin et al. (2006a,b).

The ''response'' of PV to the forcing can be seen from Fig. 5, where $C(\hat{F}, q|\tau)$ at $z = 8$ km is displayed. The basic pattern is quite simple. It is kind of a replica of the forcing pattern but shifted by ~250 km westward. At $\tau = 0$, there is a prominent maximum slightly west of the correlation point. The minimum in the east is somewhat stronger than that in the west. Motion is eastward with increasing lag. The related amplitude changes are less dramatic than in Fig. 2. The maximum amplitude at $\tau = 0$ is ~0.3 PVU and 0.15 PVU at $\tau = 1$ day. The meridional structure of the pattern is richer as in Fig. 2. The response at $z = 10$ km (Fig. 6) is quite strong with separate extrema farther north. The intensity of the maximum varies little with lag. The response pattern at $z = 6$ km (not shown) is similar to Fig. 5, but that at $z = 4$ km is too noisy and weak to be shown.

The similarity of Figs. 1 and 2b is obvious and the responses in Fig. 5 are rather close to the forcing at least as far as the patterns are concerned. On the other hand, the forcing in Fig. 2b is quite strong with a maximum amplitude of 4 PVU day^{-1}, but the observed response value of 0.3 PVU in Fig. 5b appears to be too small to be

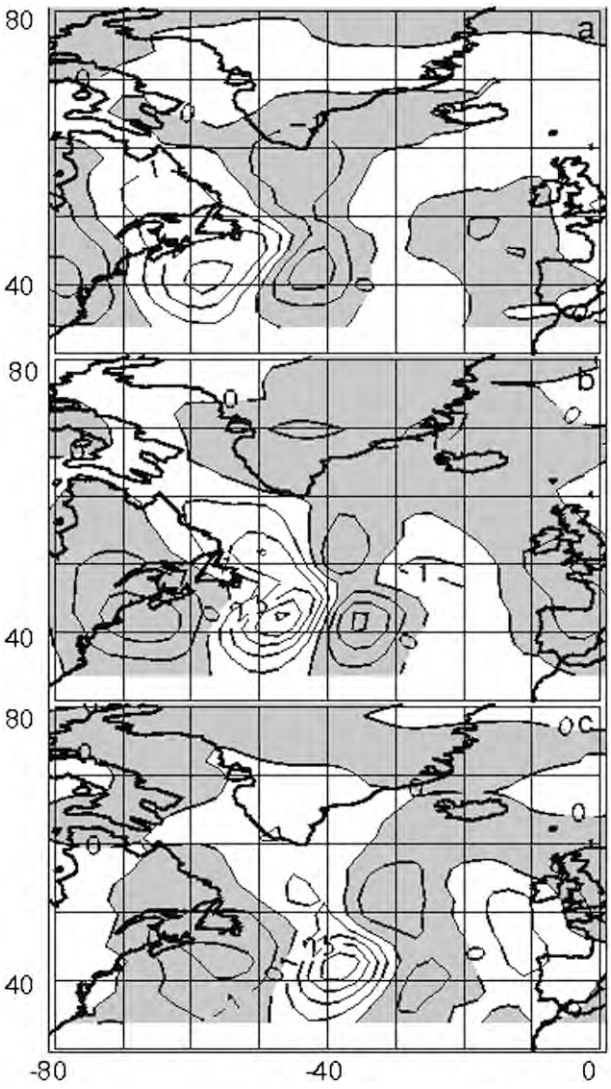

FIG. 6. As in Fig. 5, but at $z = 10$ km.

explained as a simple response to the forcing. We can test this impression by invoking an advection model where zonal advection by the mean flow is the only mechanism that affects PVU in addition to the forcing.

3. Advection model

We simplify (1.2) by discarding the meridional gradient of the mean PV. This way an advection equation results with forcing and damping. It is of obvious interest to see how much of the observed covariances $C(\hat{F}, q|\tau)$ in Figs. 5 and 6 can be explained by such an extremely simple model. Thus,

$$\frac{\partial q'}{\partial t} + \overline{U}\frac{\partial q'}{\partial x} + dq' = F(x,t) \tag{3.1}$$

is the equation to be considered where $\overline{U} > 0$ is a constant zonal mean velocity and F is now a stochastic forcing that represents the nonlinear eddy term in (1.2). Of course, (3.1) is just one-dimensional in space. Thus,

$$\left(\frac{\partial}{\partial \tau} + \overline{U}\frac{\partial}{\partial x} + d\right)C(\hat{F}, q|\tau) = C(\hat{F}, F|\tau) \tag{3.2}$$

is the equation to be solved where the right-hand side must be specified according to the observations. Given

$$D(x,\tau) = C(\hat{F}, F|\tau), \tag{3.3}$$

where D vanishes for $\tau \to \infty$, we can write down the solution

$$C(\hat{F}, q|\tau) = \int_{-\infty}^{\tau} \exp[-d(\tau - \tau')]D[x - \overline{U}(\tau - \tau'), \tau']\, d\tau'. \tag{3.4}$$

We may model the observations in Fig. 2 crudely by choosing

$$D(x,\tau) = \{[\cos(\pi\tilde{x}/2)]^3 + 3[\cos(3\pi\tilde{x}/2)]^3\}\cos(\pi\tau/2), \tag{3.5}$$

where $\tilde{x} = x - c\tau$ and coordinates in time and space are nondimensional. Moreover $D = 0$ for $|x| > 1$, $|\tau| > 1$. A scaling adapted to Fig. 2 is 1500 km for length and 2 days for time. There is a prominent maximum at $x = 0$ in (3.5) and two adjacent minima upstream and downstream. The covariances drop to 0 within the time $2/\pi$. The x integral over D vanishes, so that there is no mean forcing of PV. The eastward motion of the forcing is represented by a speed $c \sim 0.5$. That corresponds with a speed of 5 m s^{-1}, in rough agreement with the observations.

The solution is shown in Fig. 7 for a (x, τ) plane, the forcing (3.5) and a mean flow $\overline{U} = 2$ and $d = 1/2.5$ [nondimensional units; $\overline{U} = 20$ m s^{-1} and $d = 1/(5$ days) in dimensional units]. There is no response for $\tau < -1$, of course, nor for $x < -1$, but there is a rapid buildup of the standard structure with a maximum near $x = 0$ and minima upstream and downstream. The situation at $\tau = 0$ corresponds reasonably well with Fig. 5b. The pattern moves then downstream with the mean flow. There is little activity at $x > 0$ for, say, $\tau > 2$. The advection solution, however, is not satisfactory farther downstream because the decay is dictated by the damping. Atmospheric damping times are certainly not shorter than 5 days (e.g., Whitaker and Sardeshmukh 1998). The response in Fig. 7 is small for, say, $\tau \geq 3$ (i.e., after two weeks). That is too long compared to the observations.

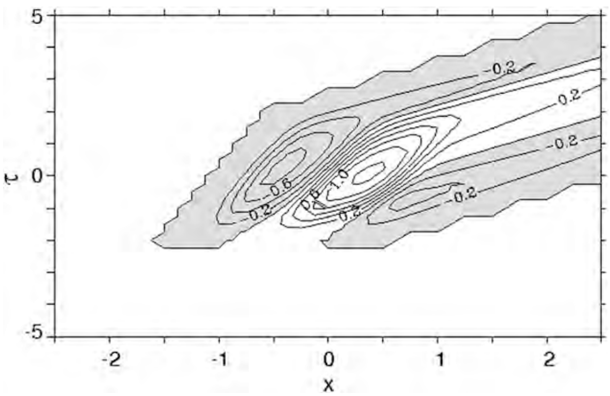

FIG. 7. Covariance $C(\hat{F}, q|\tau)$ of the forcing (3.5) at $y = 0$ and the potential vorticity as a function of nondimensional time and zonal coordinates according to (3.4) with forcing (3.5). Negative values are shaded.

The ratio of maximum response to maximum input is ~0.8 day taking into account (3.5), Fig. 7, and the scaling. The observed ratio of ~0.1 day is much smaller. One can bring down the result of the advection model somewhat by choosing specific parameter values but we have not been able to match the observations for a reasonable choice. In other words, the response in the advection model is too strong and too long-lived. Atmospheric dynamics has more possibilities to react than an advection model. This finding is in line with the result of Whitaker and Sardeshmukh (1998) that the white noise forcing provides only a minor fraction of the flow's energy. On the other hand, we can test the assumption of white noise in time by replacing $\cos(\pi\tau/2)$ by a delta function. It can be seen from (3.4) that $C(\hat{F}, q|\tau) = 0$ for $\tau < 0$. There is then a jump to the full profile of D with respect to x at $\tau = 0$. This profile moves then with speed $c + U$ downstream and is damped.

4. Discussion and conclusions

The three-dimensional divergence of the PV flux has been evaluated from data because this is the dynamic forcing needed in linear models of point-correlation maps. It is found that the autocovariance $C(\hat{F}, \hat{F}|\tau)$ shows a distinct maximum at $\tau = 0$ but the values for lags of a few days are negative and not negligible as requested by a white noise model.

The forcing is almost white in meridional direction but not zonally where pronounced up- and downstream minima are found. The extent of this wave pattern is about 3000 km. Thus the forcing has a zonally propagating structure.

The response pattern $C(\hat{F}, q|\tau)$ near $\tau = 0$ shows reasonably good agreement with that resulting from the advection equation for a forcing that mimics the observed forcing. The advective solution, however, is not acceptable for large τ and x because the observed decay cannot be captured with realistic damping rates. Moreover, the amplitudes of the response are too large. This means that the forcing is too effective in "generating" PV compared to the atmosphere. This deficit of the advection model may be explained by the fact that the advection model assumes a one-layer atmosphere without meridional PV gradients. The PV in this model responds differently to a forcing than does the atmospheric PV. On the other hand, we have to stress that although F is treated like a forcing in the paper, the divergence of the eddy PV flux is just a term in the PV equation. Nevertheless, if $C(\hat{F}, F|\tau|)$ is prescribed according to observations a satisfactory result can be expected from a solution of (1.3). If, however, $C(\hat{F}, F|\tau)$ is assumed to be white in time then we have $C(\hat{F}, q|\tau) = 0$ for $\tau < 0$ in strong contradiction to the observations. Nonlinear eddy terms should not be assumed to be white.

Our work can only be seen as a first step toward a global forcing climatology. The correlation point selected here is presumably representative of the upper tropospheric part of a storm-track region but many more points would have to be selected before a reasonably complete stochastic climatology of the forcing emerges. Moreover, no effort has been made to distinguish between resolved and subgrid motions. That is appropriate in view of the linear theories where such a separation does not make sense. It would, however, make sense if a global model is run with a certain resolution and if data with higher resolution were available. Another possibility would be the restriction of F to certain time scales. This way one could investigate, for example, the interaction of synoptic eddies and low-frequency motion (e.g., Ren et al. 2009). The ultimate step would be the incorporation of the observed forcing statistics into a linear model like that of Whitaker and Sardeshmukh (1998). In principle, the solution of the advection equation shows how this problem can be solved but one would hesitate to solve the linear equations of a global model just to obtain point-correlation maps for one grid point. A more attractive method is to analyze the forcing for many grid points and to construct a stochastic model for the forcing similar to Frederiksen and Kepert (2006) and Zidikheri and Frederiksen (2010a,b). One would have to integrate in time a global linear model with this forcing to extract the required statistics.

The calculations of the forcing covariances depend, of course, on the resolution of the data. With a grid distance of 2.25° we can be certain that the zonal structures are captured quite well. It may be, however, that the

meridional width of the forcing distribution is somewhat overestimated.

Acknowledgments. The authors thank F.-F. Jin for his constructive and encouraging comments. Remarks by two anonymous referees helped to improve the paper.

REFERENCES

Blackmon, M., V.-H. Lee, and J. Wallace, 1984: Horizontal structure of 500-mb height fluctuations with long, intermediate, and short time scales. *J. Atmos. Sci.,* **41,** 961–979.

DelSole, T., and B. Farrell, 1995: A stochastically excited linear system as a model for quasigeostrophic turbulence: Analytic results for one- and two-layer fluids. *J. Atmos. Sci.,* **52,** 2531–2547.

Egger, J., and H.-D. Schilling, 1984: Stochastic forcing of planetary-scale flow. *J. Atmos. Sci.,* **41,** 779–788.

Farrell, B., and P. Ioannou, 2009: A theory of baroclinic turbulence. *J. Atmos. Sci.,* **66,** 2444–2454.

Frederiksen, J., and S. Kepert, 2006: Dynamical subgrid-scale parameterizations from direct numerical simulations. *J. Atmos. Sci.,* **63,** 3006–3019.

Hoskins, B., and K. Hodges, 2002: New perspectives on the Northern Hemisphere winter storm tracks. *J. Atmos. Sci.,* **59,** 1041–1061.

Jin, F.-F., L.-L. Pan, and M. Watanabe, 2006a: Dynamics of synoptic eddy and low-frequency flow interaction. Part I: A linear closure. *J. Atmos. Sci.,* **63,** 1677–1694.

——, ——, and ——, 2006b: Dynamics of synoptic eddy and low-frequency flow interaction. Part II: A theory for low-frequency modes. *J. Atmos. Sci.,* **63,** 1695–1708.

Metz, W., 1986: Transient cyclone-scale vorticity forcing of blocking highs. *J. Atmos. Sci.,* **43,** 1467–1483.

Newman, M., P. Sardesmukh, and C. Penland, 1997: Stochastic forcing of the wintertime extratropical flow. *J. Atmos. Sci.,* **54,** 435–455.

Ren, H.-L., F.-F. Jin, J.-S. Kug, J. Zhao, and J. Park, 2009: A kinematic mechanism for positive feedback between synoptic eddies. *Geophys. Res. Lett.,* **36,** L11709, doi:10.1029/2009GL037294.

Whitaker, J., and P. Sardeshmukh, 1998: A linear theory of extratropical synoptic eddy statistics. *J. Atmos. Sci.,* **55,** 237–258.

Zidikheri, M., and J. Frederiksen, 2010a: Stochastic modelling of unresolved eddy fluxes. *Geophys. Astrophys. Fluid Dyn.,* **104,** 323–348.

——, and ——, 2010b: Stochastic subgrid-scale modelling for non-equilibrium geophysical flows. *Philos. Trans. Roy. Soc.,* **368A,** 145–160.